Acetylshikonin induces ferroptosis via the lipid peroxidation pathway in osteosarcoma cells

JI-YING CHEN[1,2], GUO-SHOU WANG[1,2], TSUNG-MING CHANG[3] and JU-FANG LIU[4-6]

[1]Department of Medicine, MacKay Medical College, New Taipei City 252005, Taiwan, R.O.C.; [2]Department of Orthopedic Surgery, MacKay Memorial Hospital, Taipei 104217, Taiwan, R.O.C.; [3]School of Dental Technology, College of Oral Medicine, Taipei Medical University, Taipei 110301, Taiwan, R.O.C.; [4]Translational Medicine Center, Shin-Kong Wu Ho-Su Memorial Hospital, Taipei 111045, Taiwan, R.O.C.; [5]Department of Medical Research, China Medical University Hospital, China Medical University, Taichung 404328, Taiwan, R.O.C.; [6]School of Oral Hygiene, College of Oral Medicine, Taipei Medical University, Taipei 110301, Taiwan, R.O.C.

Received November 1, 2024; Accepted September 19, 2025

DOI: 10.3892/mmr.2025.13765

Abstract. Osteosarcoma, a prevalent primary malignant bone tumor, primarily affects adolescents and young adults. Current treatment strategies involve a combination of surgical intervention and chemotherapy. However, the effectiveness of chemotherapy is constrained by considerable challenges, such as drug resistance and insensitivity. Ferroptosis, a form of programmed cell death that is distinct from apoptosis, presents a promising alternative target for cancer therapy. Ferroptosis is characterized by iron-dependent lipid peroxidation, producing reactive oxygen species (ROS) and suppressing glutathione peroxidase 4 (GPX4). Notably, ferroptosis circumvents the conventional mechanisms associated with apoptosis. Inducing ferroptosis in cancer cells may help overcome drug resistance and enhance the effectiveness of existing treatments, including chemotherapy, radiotherapy and immunotherapy. Acetylshikonin is a derivative of naphthoquinone that possesses anticancer properties. However, the effects of acetylshikonin on the treatment of osteosarcoma and the mechanisms by which it induces cancer cell death remain unclear. The present study aimed to investigate the potential of acetylshikonin to induce apoptosis in osteosarcoma cells. Using cell viability assays, ROS detection, mitochondrial membrane potential analysis and ferroptosis inhibitor rescue experiments, the results demonstrated that acetylshikonin significantly reduced the viability of osteosarcoma cell lines while exhibiting low toxicity to normal cells. Mechanistically, acetylshikonin induced the production of ROS, disrupted the mitochondrial membrane potential and promoted lipid peroxidation, ultimately leading to ferroptosis. Additionally, treatment with acetylshikonin led to decreased levels of GPX4 and increased intracellular ferrous ion (Fe^{2+}) concentrations, further supporting its role in the induction of ferroptosis. In conclusion, the current study emphasized the potential of acetylshikonin as an effective agent in inducing ferroptosis in osteosarcoma cells. Acetylshikonin reduced osteosarcoma cell viability and selectively promoted ferroptosis by increasing ROS production, disrupting mitochondrial function and enhancing lipid peroxidation. Furthermore, its ability to downregulate GPX4 and increase intracellular Fe^{2+} levels indicated its role in triggering ferroptosis. These findings suggest that acetylshikonin may be a valuable therapeutic candidate for the treatment of osteosarcoma, potentially improving outcomes and addressing the limitations of current therapies.

Introduction

Osteosarcoma is the most common primary malignant bone tumor, which predominantly affects young adults and individuals aged >60 years old. Osteosarcoma typically arises in the metaphyseal regions of long bones, including the distal femur, proximal tibia and proximal humerus (1). Despite advancements in treatment, the 5-year survival rate remains at ~60% for localized cases and 20% for metastatic disease (2,3). Conventional treatment involves a combination of surgery and chemotherapy. Surgery aims to achieve complete resection of the tumor, and chemotherapy is administered both preoperatively (as a neoadjuvant) to shrink the tumor and postoperatively (as an adjuvant) to eliminate residual disease (4). However, chemotherapy for osteosarcoma faces notable challenges, including drug resistance and the capacity of cancer cells to evade apoptosis (5). Cancer cells can evade apoptosis through various mechanisms, including the upregulation of anti-apoptotic proteins (such as Bcl-2), mutations in pro-apoptotic genes (including p53) and activation of survival pathways (6). These factors contribute to the limited long-term efficacy of chemotherapy and highlight the necessity for novel therapeutic approaches (7,8).

Ferroptosis is a programmed form of cell death that is driven by iron-dependent lipid peroxidation. Unlike apoptosis or necrosis, ferroptosis is characterized by the

Correspondence to: Professor Ju-Fang Liu, School of Oral Hygiene, College of Oral Medicine, Taipei Medical University, 250 Wuxing Street, Taipei 110301, Taiwan, R.O.C.
E-mail: jufangliu@tmu.edu.tw

Key words: osteosarcoma, acetylshikonin, ferroptosis, reactive oxygen species, glutathione peroxidase 4

accumulation of lethal lipid reactive oxygen species (ROS) and the depletion of glutathione (a crucial antioxidant) (9). Key markers of ferroptosis include the suppression of glutathione peroxidase 4 (GPX4), elevated levels of lipid peroxides and the presence of iron-dependent ROS (10,11). In cancer treatment, ferroptosis offers a promising therapeutic strategy, particularly for overcoming drug resistance. Cancer cells often develop resistance to conventional therapies by evading apoptosis; however, inducing ferroptosis can bypass these resistance mechanisms (9). Ferroptosis inducers, such as erastin and RSL3, have demonstrated effectiveness in triggering ferroptosis in various cancer cell lines, including those resistant to apoptosis (12). Additionally, ferroptosis can improve the effectiveness of treatments such as chemotherapy, radiotherapy and immunotherapy by sensitizing cancer cells to these modalities (13). Therefore, identifying natural compounds that can induce ferroptosis in cancer cells is crucial; these compounds may function as chemotherapy drugs or adjuncts, potentially improving treatment outcomes and overcoming drug resistance.

Shikonin and acetylshikonin are naphthoquinone derivatives extracted from the roots of the plant *Lithospermum erythrorhizon* (14). Shikonin has been extensively studied for its anticancer properties; it has been shown to induce apoptosis, necroptosis and ferroptosis in various cancer cell lines by generating ROS, inhibiting the EGFR and PI3K/Akt signaling pathways, and suppressing angiogenesis (15). Via these mechanisms, shikonin also enhances the efficacy of conventional therapies such as chemotherapy and radiotherapy by sensitizing cancer cells to these treatments (15). Acetylshikonin shares similar anticancer mechanisms, but has shown distinct advantages in certain contexts. The acetylation of shikonin enhances its stability and bioavailability, facilitating more effective delivery and sustained action within the body (15). This modification enhances its ability to induce apoptosis and inhibit cancer cell proliferation. Additionally, acetylshikonin has been identified as a novel tubulin polymerization inhibitor, demonstrating marked antitumor activity in hepatocellular carcinoma (16). Furthermore, ROS production from acetylshikonin is associated with upregulation of apoptosis pathways in osteosarcoma cells (17). These properties indicate that acetylshikonin may be a promising candidate for cancer treatment, with potential applications in overcoming drug resistance and improving the efficacy of existing therapies. However, the mechanism underlying the ability of acetylshikonin to induce cell death in osteosarcoma remains poorly understood. The present study aimed to investigate whether acetylshikonin induces ferroptosis in osteosarcoma cells and to elucidate the underlying mechanisms, thereby assessing its potential as a novel therapeutic agent.

Materials and methods

Chemicals. Primary antibodies against GPX4 (cat. no. GTX03194), Bcl-2 (cat. no. GTX100064), Bcl-xl (cat. no. GTX637939), Bak (cat. no. GTX100063), Bax (cat. no. GTX109683) and β-actin (cat. no. GTX109639) were acquired from GeneTex, Inc. The secondary HRP-conjugated anti-rabbit monoclonal (cat. no. sc-2357) antibody was purchased from Santa Cruz Biotechnology, Inc. The other chemicals and reagents used in the present study were obtained from MilliporeSigma, unless otherwise specified.

Cell culture. U2OS is an epithelial-like osteosarcoma cell line originally derived from the tibial tumor of a 15-year-old Caucasian female patient. This cell line exhibits a hypertriploid karyotype with extensive chromosomal rearrangements, including stable marker chromosomes involving chromosomes 1, 7, 9 and 17. HOS is a fibroblast- and epithelial-like cell line established from the osteosarcoma lesion of a 13-year-old Caucasian female patient. This cell line displays a flat morphology, low saturation density and is highly sensitive to transformation. MG63 is a fibroblast-like osteosarcoma cell line derived from the bone of a 14-year-old Caucasian male patient. This cell line is hypotriploid with a modal chromosome number of 66, and it consistently exhibits 18-19 marker chromosomes. All cell lines were authenticated using short tandem repeat profiling. The human osteosarcoma cell lines (U2OS, HOS and MG63) and normal human osteoblasts (hFOB 1.19) were sourced from the American Type Culture Collection. Osteosarcoma cells were maintained in Dulbecco's Modified Eagle Medium (DMEM) supplemented with 10% fetal bovine serum, 100 U/ml penicillin and 100 μg/ml streptomycin. hFOB 1.19 cells were cultured in a 1:1 mixture of Ham's F-12 Medium and DMEM supplemented with 2.5 mM L-glutamine (without phenol red), as per the supplier recommendations. All cells were incubated at 37˚C in a humidified atmosphere with 5% CO_2.

Cell viability assays. The hFOB 1.19, U2OS, HOS and MG63 cells were seeded in 48-well plates at a density of $1x10^4$ cells/well and were allowed to adhere overnight. The U2OS, HOS and MG63 cells were then exposed to various concentrations (0, 0.05, 0.1, 0.5, 1, 3, 10 and 20 μM) of acetylshikonin (cat. no. HY-N2181; MedChemExpress) for 24 or 48 h at 37˚C. The hFOB 1.19 cell line was exposed to different concentrations (0, 0.1, 0.5, 1 and 3 μM) of acetylshikonin for 24 h at 37˚C. Untreated cells were used as controls. Cell viability was determined using the Cell Counting Kit-8 (CCK-8; cat. no. 96992; MilliporeSigma), according to the manufacturer's instructions. Absorbance was measured at 450 nm using a microplate reader (BioTek; Agilent Technologies, Inc.).

In addition, U2OS, HOS, and MG63 cells were seeded at $5x10^4$ cells/well on glass coverslips in 24-well plates and treated with acetylshikonin. (0, 0.5, 1, 2.5, 5 and 10 μM) for 24 h at 37˚C. After treatment, the cells were stained with Hoechst 33342 (5 μg/ml), Calcein-AM (2 μM) and propidium iodide (PI; 1 μg/ml) at 37˚C for 30 min. Hoechst 33342 stained all nuclei (blue fluorescence), Calcein-AM stained viable cells (green fluorescence), and PI identified dead cells with compromised membranes (red fluorescence). Untreated cells were used as controls. Furthermore, cells treated with acetylshikonin (0 and 3 μM) for 24 h at 37˚C were observed using a Nikon Eclipse Ti fluorescence microscope (Nikon Corporation) to evaluate changes in morphology and cell density.

To validate the involvement of ferroptosis, U2OS, HOS and MG63 cells were pretreated with ferrostatin-1 (1 μM; a ferroptosis inhibitor; cat. no. SML0583; Sigma-Aldrich; Merck KGaA) or liproxstatin-1 (1 μM; a ferroptosis inhibitor;

cat. no. SML1414; Sigma-Aldrich; Merck KGaA) for 1 h, followed by treatment with acetylshikonin (3 μM) for 24 h at 37˚C. Cell viability was assessed using the CCK-8 assay, as aforementioned. For comparative analysis, cells were also treated with erastin (3 μM; a ferroptosis inducer; cat. no. E7781; Sigma-Aldrich; Merck KGaA) or RSL3 (3 μM; a ferroptosis inducer; cat. no. SML2234; Sigma-Aldrich) for 24 h at 37˚C, and cell viability was measured using the same method. To differentiate ferroptosis from apoptosis and necroptosis, osteosarcoma cells (MG63, HOS and U2OS) were pretreated with the caspase-3 inhibitor z-DEVD-FMK (10 μM; cat. no. 264155; Sigma-Aldrich), the RIPK1 inhibitor necrostatin-1 (10 μM; cat. no. 480065; Sigma-Aldrich) or the necrosis inhibitor IM-54 (10 μM; cat. no. SML0412; Sigma-Aldrich) for 1 h prior to treatment with acetylshikonin (3 μM) for 24 h at 37˚C. Untreated cells were used as controls. Cell viability was subsequently assessed using the CCK-8 assay, as aforementioned. All experiments were conducted in quadruplicate (n=4) to ensure reproducibility.

DNA fragmentation analysis. TUNEL enzymatically labels the 3'-ends of fragmented DNA, a hallmark of apoptosis, using a fluorophore-conjugated nucleotide (18,19). DNA damage was analyzed using the TUNEL assay (BD Biosciences). Briefly, cells were treated with acetylshikonin (0, 0.1, 0.25, 0.5, 1 and 3 μM) for 24 h at 37˚C, followed by fixation with 4% paraformaldehyde in PBS (pH 7.4) for 60 min at room temperature and permeabilization with 0.1% Triton X-100 in 0.1% sodium citrate on ice for 2 min. TUNEL labeling was then performed with the reaction mixture containing fluorescein-dUTP at 37˚C for 60 min in a humidified dark chamber. Finally, DNA strand breaks were detected using a flow cytometer (Accuri C5; BD Biosciences), and flow cytometry data were acquired and analyzed using BD Accuri C6 Software (version 227.4; BD Biosciences).

Analysis of apoptotic and necrotic cells. To assess apoptotic and necrotic cell populations, Annexin V/PI staining was performed using an apoptosis detection kit (cat. no. APOAF; Sigma-Aldrich; Merck KGaA). Briefly, cells were seeded at a density of $5x10^5$ cells/well in 6-well plates and treated with acetylshikonin at 0, 0.1, 0.25, 0.5, 1 or 3 μM for 24 h at 37˚C. Cells were then stained with 1 μg/ml PI and 0.5 μg/ml FITC-conjugated Annexin V for 15 min at 37˚C, and analyzed by flow cytometry (Accuri C5; BD Biosciences). Flow cytometry data were acquired and analyzed using BD Accuri C6 Software (version 227.4; BD Biosciences). For ferroptosis inhibition experiments, cells were pretreated with ferrostatin-1 (10 μM) for 1 h at 37˚C prior to acetylshikonin treatment (3 μM) for 24 h at 37˚C.

Cell cycle analysis. Cells were seeded in 6-well plates at a density of $5x10^5$ cells/well and treated with acetylshikonin (0, 0.1, 0.5, 1 and 3 μM) for 24 h at 37˚C. After treatment, the cells were fixed with 75% ethanol at -20˚C for ≥2 h. After washing, the cells were stained with PI solution (0.1% Triton X-100, 0.2 mg/ml RNase A (cat. no. 70856; Merck KGaA), 10 μg/ml PI (cat. no. P4170; Sigma-Aldrich; Merck KGaA) for 30 min at 37˚C and analyzed using flow cytometry (Accuri C5; BD Biosciences). Untreated cells were used as controls. Flow cytometry data were acquired and analyzed using BD Accuri C6 Software (version 227.4; BD Biosciences).

Cellular ROS assay. H_2DCFDA (Thermo Fisher Scientific, Inc.) is a non-fluorescent compound that, after intracellular deacetylation, emits green fluorescence upon oxidation by ROS (excitation ~511 nm, emission ~533 nm). Intracellular ROS levels were determined using H_2DCFDA in the present study. Cells ($5x10^5$) were treated with acetylshikonin (0, 0.1, 0.25, 0.5, 1 and 3 μM) for 1 h at 37˚C, followed by incubation with 1 μM H_2DCFDA at 37˚C for 30 min. Untreated cells were used as controls. ROS levels were analyzed via flow cytometry (Accuri C5; BD Biosciences). Flow cytometry data were acquired and analyzed using BD Accuri C6 Software (version 227.4; BD Biosciences).

Analysis of mitochondrial membrane potential. Mitochondrial membrane potential was assessed using the cationic dye JC-1 (Thermo Fisher Scientific, Inc.); in healthy mitochondria, it forms red-fluorescent J-aggregates, whereas in depolarized or apoptotic mitochondria, JC-1 remains in a monomeric form, emitting green fluorescence. Briefly, cells were incubated with acetylshikonin (0 and 1 μM) for 2 or 8 h and were subsequently stained with JC-1 (5 μg/ml) for 30 min at 37˚C. Untreated cells were used as controls. Fluorescence intensity was observed using a Nikon Eclipse Ti fluorescence microscope (Nikon Corporation).

Western blotting. Cells were seeded at a density of $5x10^5$ cells/well in 6-well plates and treated with acetylshikonin (0, 0.1, 0.5, 1, and 3 μM) for 24 h at 37˚C. After treatment, the cells were lysed with RIPA buffer [50 mM Tris-HCl (pH 7.4), 150 mM NaCl, 1% NP-40, 0.25% sodium deoxycholate, 0.1-2% SDS], supplemented with a protease inhibitor mix (1 mM PMSF, 10 ng/ml leupeptin, 1 ng/ml aprotinin). Protein concentration was determined using the BCA Protein Assay Kit (cat. no. 71285-M; Merck KGaA). Equal amounts of protein (50 μg/lane) were loaded and separated by SDS-PAGE on 15% gels, followed by transfer to PVDF membranes (MilliporeSigma). Membranes were blocked with 5% non-fat milk in TBS-0.05% Tween-20 for 1 h at room temperature and incubated overnight at 4˚C with primary antibodies (1:1,000 dilution). After washing, the membranes were incubated with HRP-conjugated secondary antibodies (1:10,000 dilution) for 1 h at room temperature. Protein bands were visualized using an enhanced chemiluminescence detection system (Analytik Jena US, LLC).

Transmission electron microscopy analysis. Following treatment with acetylshikonin (0 and 3 μM) for 24 h at 37˚C, HOS cells ($5x10^5$) were collected, fixed in 70% Karnovsky fixative at 4˚C, and processed for ultrastructural examination. Samples were dehydrated through a graded ethanol series, embedded in Epon 812 resin (polymerized at 60˚C for 48 h) and sectioned into ultrathin slices (70-90 nm) using an ultramicrotome. Sections were stained with 2% uranyl acetate for 20 min at room temperature, followed by Reynolds's lead citrate for 10 min at room temperature. Images were obtained using a JEOL JEM-1400 transmission electron microscope (JEOL, Ltd.).

Analysis of lipid peroxidation. C11-BODIPY™ 581/591 (Thermo Fisher Scientific, Inc.) is a lipid peroxidation sensor dye that shifts its fluorescence from red (~590 nm) to green (~510 nm) upon oxidation. Imaging and quantification of C11-BODIPY 581/591 staining were performed using fluorescence microscopy and flow cytometry in the current study. Briefly, cells ($5x10^4$) were incubated with acetylshikonin (0, 0.1, 0.3, 1 and 3 μM for 30 min at 37˚C and C11 BODIPY dye at 37˚C for 30 min. Lipid peroxidation was subsequently determined based on fluorescence shifts from 591 nm (non-oxidized) to 510 nm (oxidized) using fluorescence microscopy and flow cytometry (Accuri C5; BD Biosciences). Untreated cells were used as controls. Flow cytometry data were acquired and analyzed using BD Accuri C6 Software (version 227.4; BD Biosciences).

Analysis of intracellular ferrous ion (Fe^{2+}) concentrations. Osteosarcoma cells (HOS, MG63 and U2OS) were treated with acetylshikonin (0 and 3 μM) for 24 h at 37˚C. After treatment, the cells were lysed with the buffer solution provided in the Fe^{2+} Colorimetric Assay Kit (cat. no. E-BC-K881-M; Elabscience Bionovation Inc.), which contains Tris-based buffer components, according to the manufacturer's protocol. For each assay, $1x10^6$ cells were lysed in 200 μl buffer on ice for 10 min with gentle mixing every 5 min. Lysates were centrifuged at 15,000 x g for 10 min at 4˚C, and the supernatant was incubated with the Fe^{2+} detection reagent for 30 min at room temperature. Untreated cells were used as controls. Absorbance was measured at 593 nm using a microplate reader (Thermo Fisher Scientific, Inc.).

Statistical analysis. Data are presented as the mean ± SD from at least four independent experiments. Statistical comparisons between groups were conducted using one-way ANOVA followed by Tukey's post-hoc test. $P<0.05$ was considered to indicate a statistically significant difference.

Results

Acetylshikonin reduces the viability of osteosarcoma cell lines and enhanced membrane permeability. The present study first assessed the effect of acetylshikonin (Fig. 1A) on the viability of both normal osteoblasts (hFOB 1.19) and osteosarcoma cells. After treating hFOB 1.19 cells with acetylshikonin (0.5-3 μM) for 24 h, cell viability remained at ~80% (Fig. 1B), indicating low toxicity in normal cells. By contrast, the IC_{50} values for MG63, HOS and U2OS osteosarcoma cells after 24 h of treatment with acetylshikonin (0.5-20 μM) were 0.45, 0.83 and 0.69 μM, respectively (Fig. 1C-E). After 48 h of treatment, the IC_{50} values decreased to 0.40, 0.28 and 0.17 μM, respectively. In addition, phase-contrast microscopy revealed a marked reduction in the confluence of osteosarcoma cell lines following acetylshikonin (3 μM) treatment (Fig. 1F). Hoechst 33342 staining also showed a marked decrease in the number of MG63, HOS and U2OS cells after treatment with acetylshikonin (0.5-10 μM). Hoechst 33342 staining revealed dose-dependent increases in apoptotic nuclear condensation (brighter, punctate nuclei) in U2OS cells treated with acetylshikonin, which is associated with reduced cell viability (Fig. 1G). Additionally, acetylshikonin enhanced the uptake of PI dye into cells in a dose-dependent manner, indicating compromised cell membrane integrity. Calcein-AM staining further confirmed that acetylshikonin notably reduced the viability of osteosarcoma cells. These results indicated that acetylshikonin has a potent cytotoxic effect on osteosarcoma cell lines, primarily through mechanisms associated with cell permeability. Notably, acetylshikonin demonstrates low toxicity to normal cells, highlighting its potential as a promising therapeutic agent for osteosarcoma treatment.

Acetylshikonin induces DNA fragmentation and cell death in osteosarcoma cells. To elucidate the mechanism by which acetylshikonin affects osteosarcoma cell viability, MG63, HOS and U2OS cells were treated with acetylshikonin (0.1-3 μM) for 24 h, and DNA fragmentation was assessed using the TUNEL assay. A significant increase in DNA fragmentation was observed in all three cell lines following treatment with acetylshikonin (Fig. 2). Treatment with 3 μM acetylshikonin significantly increased the percentage of TUNEL-positive cells compared with that in the untreated control group.

Flow-cytometric apoptosis profiling after 24 h of acetylshikonin treatment (0.0-0.5 μM) showed increases in upper-right (UR; Annexin V^+/PI^+) and upper-left (UL; PI^+ only) quadrant populations. In particular, following treatment with 0.5 μM acetylshikonin, in MG63 cells, the percentage of UL quadrant cells increased from 0.7 to 9.8% and UR quadrant cells increased from 4.0 to 5.7%); in HOS cells the percentage of UL quadrant cells increased from 2.4 to 10.4% and UR quadrant cells increased from 0.1 to 1.0%; and in U2OS cells the percentage of UL quadrant cells increased from 3.1 to 12.6% and UR quadrant cells increased from 3.4 to 3.8%, these findings indicated that the cells were undergoing apoptosis. By contrast, at higher doses (1-3 μM), the major population shifted to PI^+/Annexin V^- cells in the UL quadrant, with a concomitant decrease in Annexin V^+/PI^+ cells in the UR quadrant, indicating a dose-dependent increase in necrotic cell death rather than late apoptosis/secondary necrosis (Fig. 3). Quantification in Fig. 3 was performed by combining Annexin V^+/PI^+ and Annexin V^-/PI^+ populations. Statistical analysis showed that acetylshikonin treatment at 1-3 μM significantly increased the proportion of PI^+ cells , mainly due to the enhanced Annexin V^-/PI^+ population.

The current study also examined the effect of acetylshikonin on cell cycle distribution. Acetylshikonin treatment significantly increased the number of sub-G_1 cells, indicative of DNA fragmentation, and decreased the number of G_0/G_1 cells in osteosarcoma cell lines (Fig. 4). A significant increase in the sub-G_1 population was observed in all cell lines following 3 μM acetylshikonin treatment. Taken together, the increase in DNA fragmentation (TUNEL assay), the predominance of PI^+ cells at higher doses (Annexin V/PI analysis), and the accumulation of sub-G_1 cells (cell cycle analysis) indicated that acetylshikonin may disrupt cellular integrity and induce cell death in osteosarcoma cells through mechanisms that may differ from conventional apoptosis.

Acetylshikonin induces ROS production and loss of mitochondrial membrane potential. Given the established anticancer effects of ROS generation induced by shikonin and

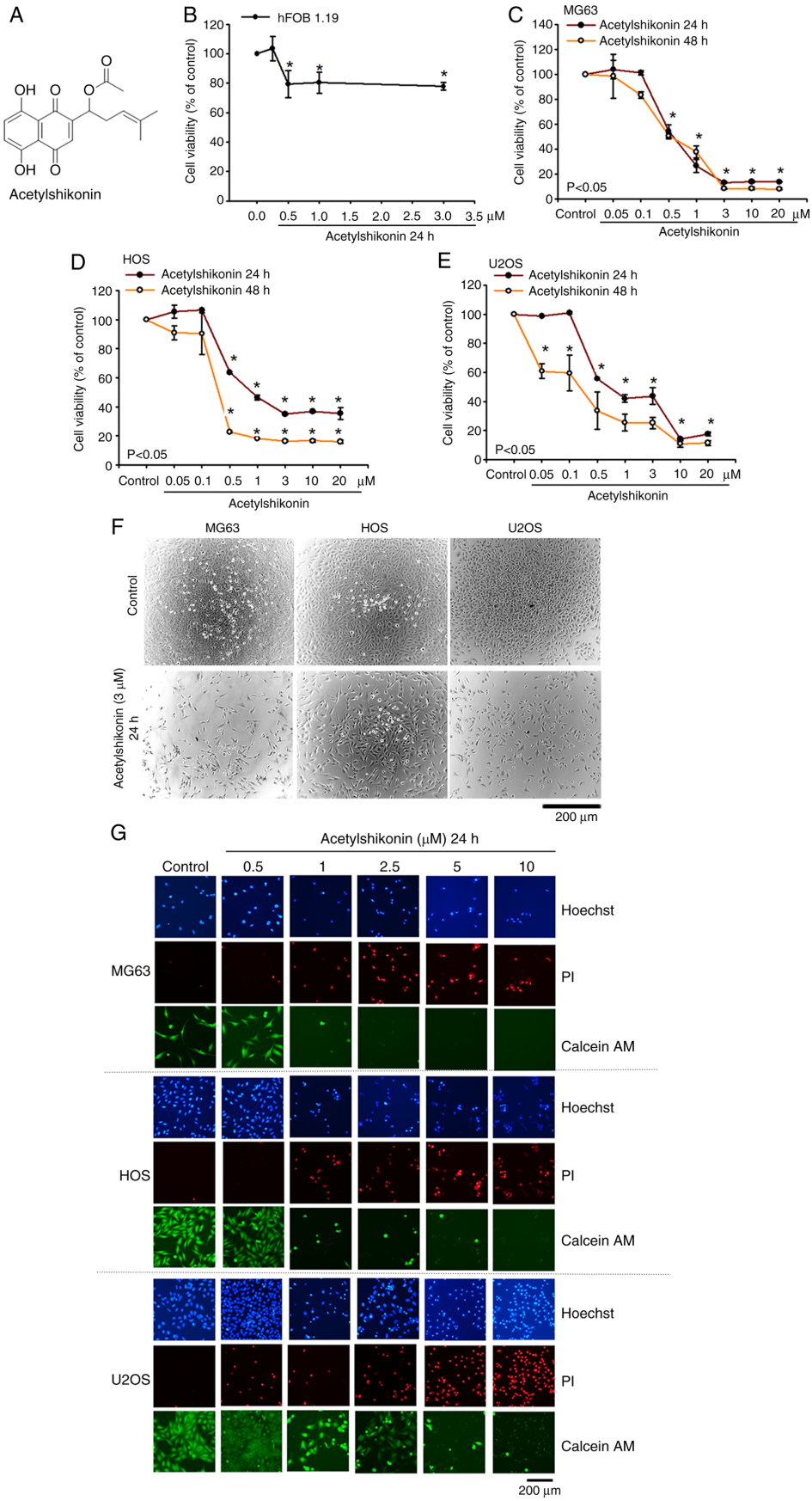

Figure 1. Acetylshikonin reduces osteosarcoma cell viability and increases membrane permeability. (A) Molecular structure of acetylshikonin. (B) CCK-8 assay results showing the viability of hFOB 1.19 cells following exposure to acetylshikonin (0.5-3 μM) for 24 h (n=4). (C) MG63, (D) HOS and (E) U2OS cell viability was assessed using the CCK-8 assay following treatment with acetylshikonin (0.05-20 μM) for 24 and 48 h (n=4). (F) Phase-contrast microscopy images depicting morphological changes in osteosarcoma cells treated with acetylshikonin (3 μM) for 24 h (n=4). (G) Fluorescence microscopy images showing nuclear staining with Hoechst 33342, membrane integrity with PI and viability with Calcein-AM in osteosarcoma cells treated with acetylshikonin (0.5-10 μM) for 24 h (n=4). Data are presented as the mean ± SD. *P<0.05 vs. untreated control. CCK-8, Cell Counting Kit-8; PI, propidium iodide.

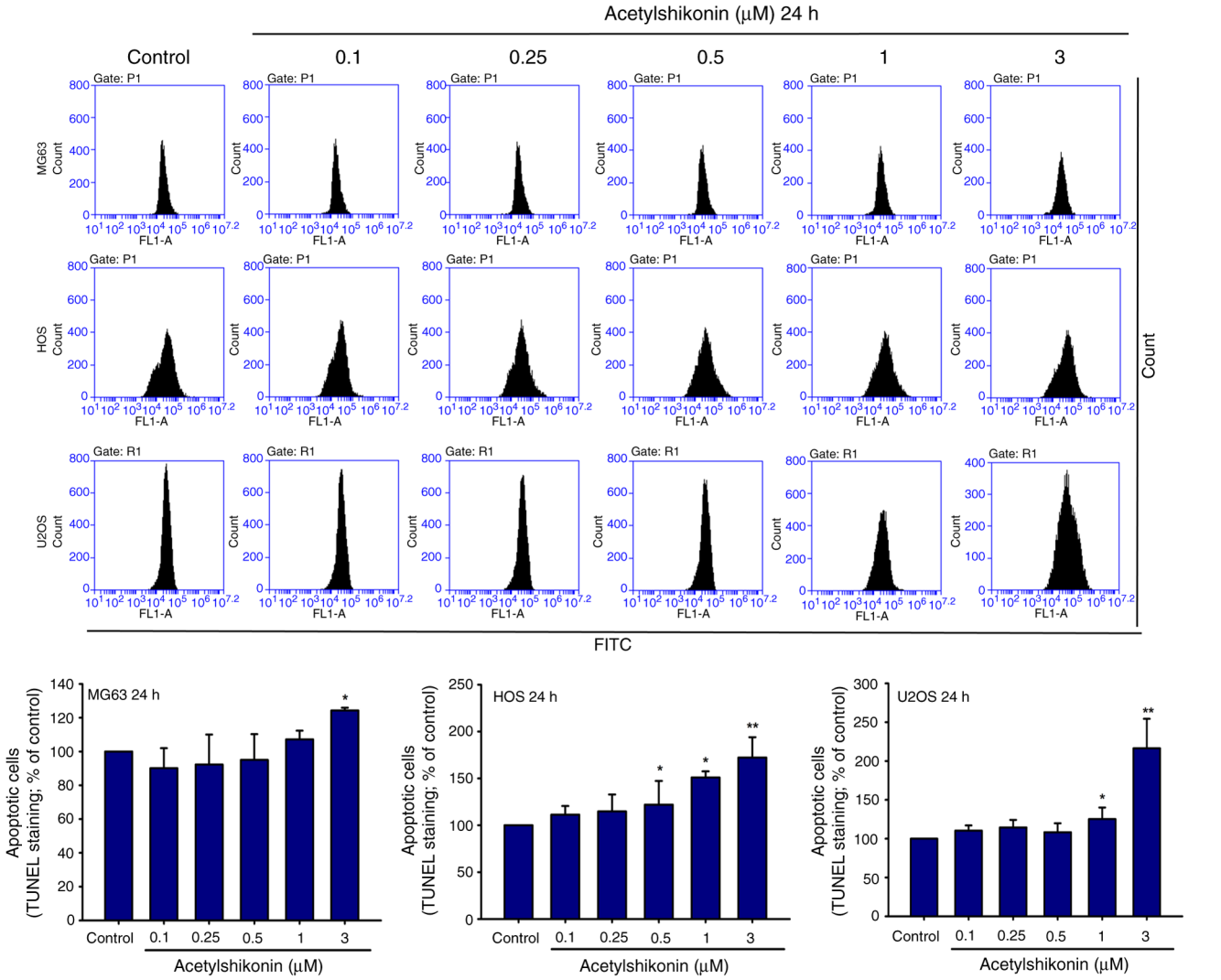

Figure 2. Acetylshikonin induces DNA fragmentation in osteosarcoma cells. Osteosarcoma cells ($5x10^5$) were treated with acetylshikonin (0.1-3 μM) for 24 h, then underwent the TUNEL assay. Fluorescence was analyzed by flow cytometry (n=4). Untreated cells were used as controls. Data are presented as the mean ± SD. *P<0.05, **P<0.01 vs. untreated control.

acetylshikonin in various cancer cells (15,17), the current study investigated the effect of acetylshikonin on intracellular ROS levels in osteosarcoma cells. Treatment with acetylshikonin at 0.5-3 μM resulted in a significant increase in ROS production in osteosarcoma cell lines (Fig. 5). Acetylshikonin at 3 μM significantly increased intracellular ROS levels compared with those in the untreated control group (P<0.01). This increase in ROS may be strongly associated with cell death and mitochondrial dysfunction (20,21). The present study next examined how acetylshikonin influences mitochondrial membrane potential in osteosarcoma cells to further elucidate its effects on mitochondrial function. Administration of acetylshikonin (1 μM) disrupted the mitochondrial membrane potential, assessed by fluorescence microscopy, as indicated by a reduction in JC-1 red fluorescence (Fig. 6A and B). A marked reduction in mitochondrial membrane potential, indicated by the JC-1 red/green fluorescence ratio, was observed after acetylshikonin treatment.

Furthermore, western blot analysis revealed that acetylshikonin treatment increased the levels of pro-apoptotic proteins Bax and Bak, which regulate mitochondrial membrane permeability, while decreasing the expression levels of anti-apoptotic proteins Bcl-2 and Bcl-xl (Fig. 6C). These results suggested that acetylshikonin induces osteosarcoma cell death through ROS generation and the loss of mitochondrial membrane potential, which may be associated with apoptosis. However, additional experimental data are required to fully elucidate the underlying mechanisms.

Acetylshikonin induces ferroptosis in osteosarcoma cells. Mitochondria are the primary generators of intracellular ROS and serve a crucial role in regulating iron homeostasis (22). Using transmission electron microscopy, the effect of acetylshikonin on mitochondrial morphology was observed in osteosarcoma cells. Treatment with acetylshikonin reduced mitochondrial volume without inducing cell swelling or shrinkage, which are morphological characteristics of ferroptosis (Fig. 7A) (22). The current study further investigated whether acetylshikonin induces lipid peroxidation in osteosarcoma cell lines. Fluorescence microscopy and flow cytometry revealed that acetylshikonin (1-3 μM) significantly induced lipid peroxidation, as evidenced by the shift

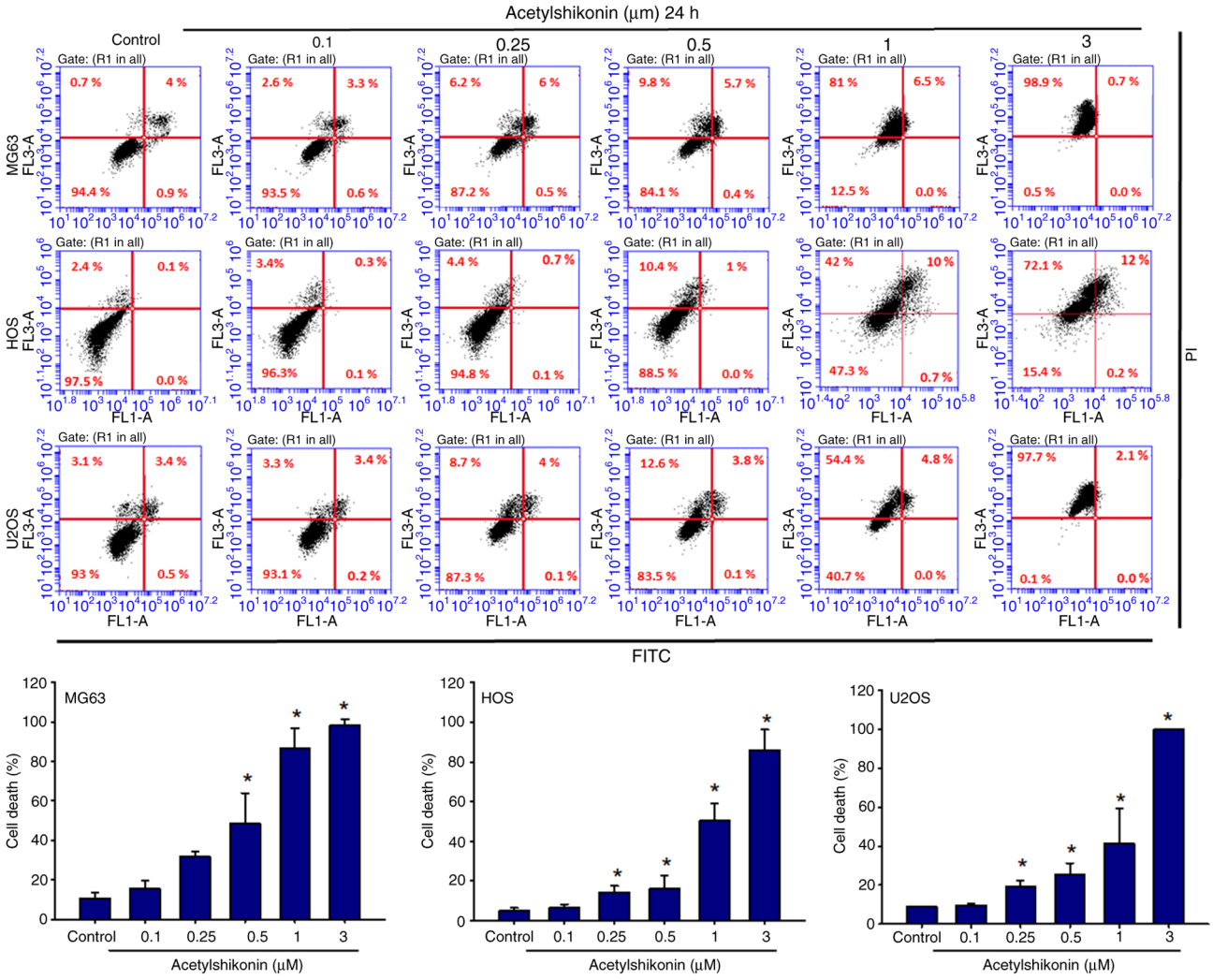

Figure 3. Acetylshikonin induces apoptosis in osteosarcoma cells. Osteosarcoma cells ($5x10^5$) were treated with acetylshikonin (0.1-3 μM) for 24 h, then underwent the Annexin V/PI assay (n=4). Untreated cells were used as controls. Data are presented as the mean ± SD. *P<0.05 vs. untreated control. PI, propidium iodide.

in BODIPY dye fluorescence from red to green (Fig. 7B-E). Treatment with 3 μM acetylshikonin significantly increased lipid peroxidation, as indicated by enhanced green fluorescence of C11-BODIPY compared with that in the control group. Additionally, treatment with acetylshikonin (3 μM) significantly increased intracellular Fe^{2+} concentrations in osteosarcoma cells compared with those in untreated cells (Fig. 7F-H). The present study also observed a reduction in GPX4 protein expression in acetylshikonin-treated osteosarcoma cells compared with that in the untreated control group, as shown by western blotting (Fig. 7I-K). These findings suggested that acetylshikonin induces osteosarcoma cell death through mechanisms involving mitochondrial size reduction, lipid peroxidation and a decrease in GPX4 levels, which are indicative of ferroptosis.

To further confirm that acetylshikonin-induced cell death is ferroptosis-dependent, the current study compared the protective effects of two ferroptosis inhibitors, ferrostatin-1 and liproxstatin-1. Pretreatment with either ferrostatin-1 (1 μM) or liproxstatin-1 (1 μM) for 1 h significantly reversed the reduction in cell viability caused by acetylshikonin (3 μM) in osteosarcoma cells (Fig. 8A-C). To rigorously exclude apoptosis and necroptosis as alternative cell-death pathways, cells were treated with the caspase-3 inhibitor z-DEVD-FMK, the RIPK1 inhibitor necrostatin-1 and the necrosis inhibitor IM-54. None of these inhibitors rescued acetylshikonin-induced cytotoxicity (Fig. 8A-C). These results provide additional pharmacological evidence that the cell death induced by acetylshikonin is mediated through ferroptosis. Similar results were observed in flow cytometry with Annexin V/PI staining. Treatment with acetylshikonin markedly increased the proportion of PI^+ cells, calculated as the combined Annexin V^+/PI^+ and Annexin V^-/PI^+ populations, whereas pretreatment with ferrostatin-1 significantly reduced this PI^+ population in osteosarcoma cell lines (Fig. 8D). Although the reduction was mainly attributable to a decrease in Annexin V^-/PI^+ cells, this subset was not analyzed statistically on its own. Additionally, the cytotoxic potency of acetylshikonin was compared with two classical ferroptosis inducers, erastin and RSL3. Treatment with erastin (3 μM) or RSL3 (3 μM) for 24 h resulted in a significant decrease in cell viability, similar in magnitude to that caused by acetylshikonin (Fig. 8E). These findings indicated that acetylshikonin exhibits ferroptosis-inducing activity comparable to established inducers, further reinforcing its potential

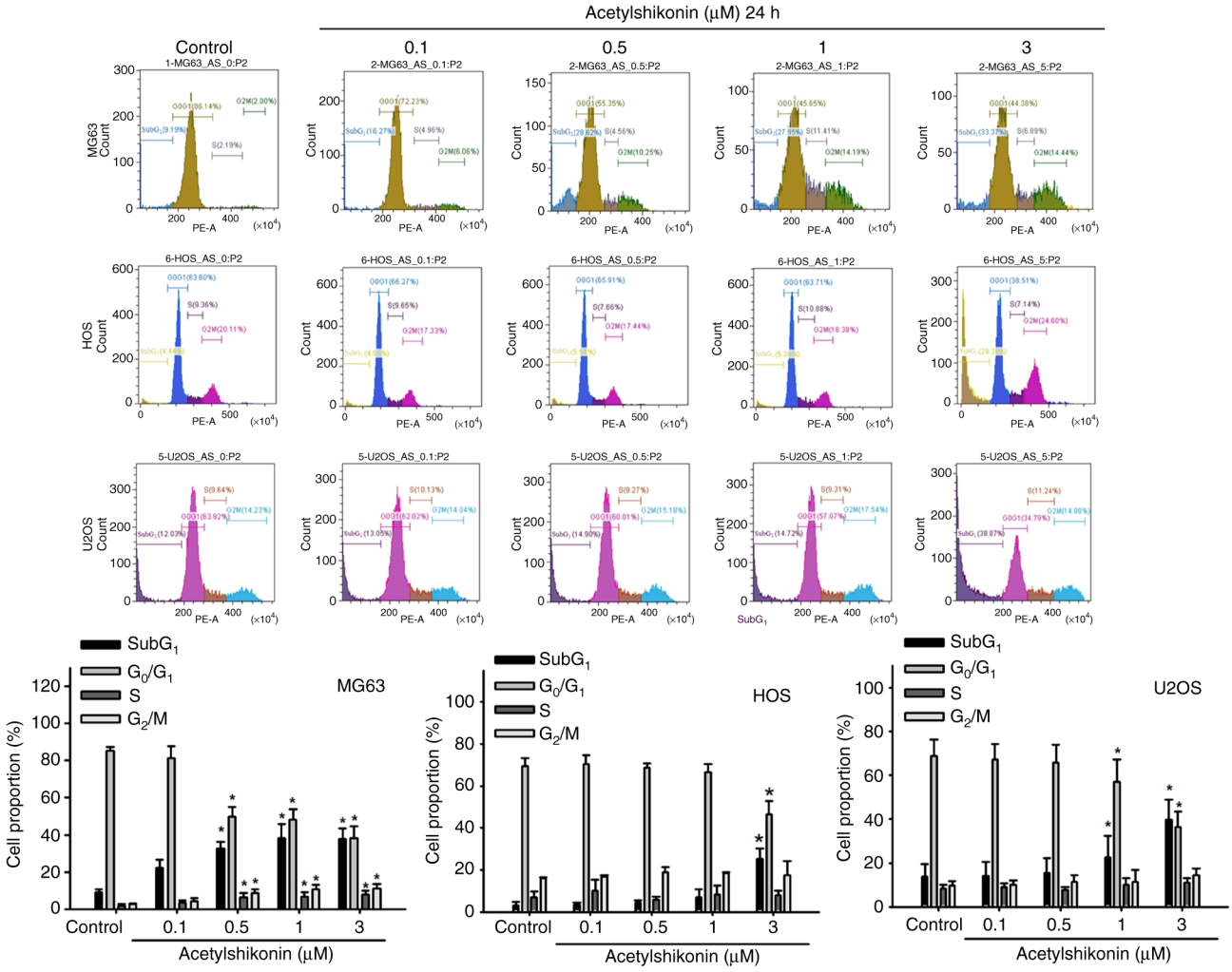

Figure 4. Acetylshikonin promotes cell cycle arrest in osteosarcoma cells. Cell cycle distribution of osteosarcoma cells treated with acetylshikonin (0.1-3 μM) for 24 h, was assessed by propidium iodide staining and flow cytometry. Untreated cells were used as controls. Data are presented as the mean ± SD. *P<0.05 vs. untreated control.

as a therapeutic ferroptosis activator in osteosarcoma cells. These results experimentally demonstrated that acetylshikonin induces ferroptosis in osteosarcoma cells. This form of cell death is distinct from classic necrosis and apoptosis, highlighting the potential of acetylshikonin as a novel therapeutic agent targeting ferroptosis in osteosarcoma cells.

Discussion

The present study investigated the potential of acetylshikonin to induce cell death in osteosarcoma cells. The results demonstrated that acetylshikonin significantly reduced the viability of osteosarcoma cell lines while exhibiting low toxicity to normal cells. Mechanistically, acetylshikonin induced ROS production, disrupted the mitochondrial membrane potential and promoted lipid peroxidation, ultimately leading to ferroptosis. Additionally, treatment with acetylshikonin resulted in decreased levels of GPX4 and increased intracellular Fe^{2+} concentrations, further supporting its role in the induction of ferroptosis. These findings suggested that acetylshikonin may address the limitations of conventional chemotherapy by targeting ferroptosis, a unique form of cell death. This highlights the potential of acetylshikonin as a promising therapeutic agent for osteosarcoma, offering a novel treatment option that could enhance patient outcomes and address the limitations of current chemotherapy.

Chemotherapeutic agents have long been a cornerstone of cancer treatment, which primarily function by inducing apoptosis in cancer cells. However, their efficacy is frequently hindered by substantial challenges, including drug resistance and severe side effects (23,24). The development of drug resistance and the ability of cancer cells to evade apoptosis represent key adaptations that ultimately result in treatment failure and disease progression (23,24). Ferroptosis, a form of programmed cell death that is distinct from apoptosis, presents a promising alternative target for cancer therapy. Characterized by elevated lipid peroxides dependent on iron, the production of ROS and the suppression of GPX4, ferroptosis circumvents the conventional mechanisms associated with apoptosis (9,12,25,26). Inducing ferroptosis in cancer cells can help overcome drug resistance and enhance the effectiveness of existing treatments, including chemotherapy, radiotherapy and immunotherapy (9,12). The current findings are consistent with these concepts, and notably,

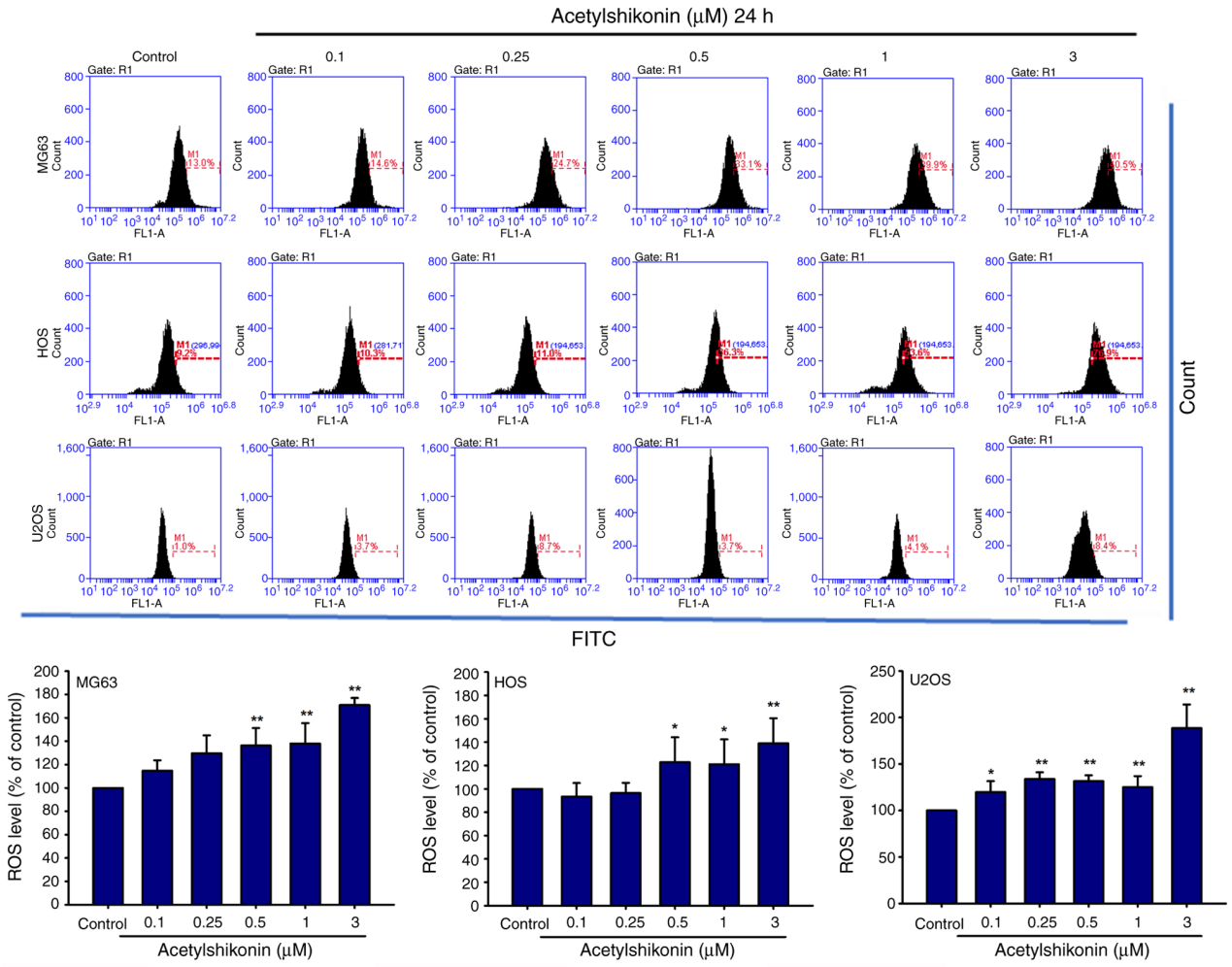

Figure 5. Acetylshikonin promotes intracellular ROS accumulation. Osteosarcoma cells ($5x10^5$) were treated with acetylshikonin (0.1-3 μM) for 1 h, then stained with 1 μM H_2DCFDA. Fluorescence was analyzed by flow cytometry (n=4). Untreated cells served as controls. Data are presented as the mean ± SD. *P<0.05, **P<0.01 vs. untreated control. ROS, reactive oxygen species.

acetylshikonin-induced ferroptosis was further confirmed by the reversal of cell death following treatment with ferrostatin-1, underscoring the critical involvement of ferroptosis processes in acetylshikonin-mediated cytotoxicity.

To further distinguish ferroptosis from other forms of regulated cell death, inhibitor rescue assays were performed using the caspase-3 inhibitor z-DEVD-FMK (apoptosis), the RIPK1 inhibitor necrostatin-1 (necroptosis) and the necrosis inhibitor IM-54 across three osteosarcoma cell lines. None of these inhibitors significantly reversed the cytotoxic effects of acetylshikonin. By contrast, ferrostatin-1 conferred substantial protection. These findings strengthen the conclusion that acetylshikonin-induced cell death is mediated through a ferroptosis-specific mechanism rather than apoptosis or necroptosis. These findings suggest that acetylshikonin may address the limitations of conventional chemotherapy by targeting ferroptosis, thereby providing a novel approach for treating osteosarcoma.

Shikonin, a naphthoquinone derivative derived from *Lithospermum erythrorhizon*, has demonstrated notable anticancer properties against various types of cancer, including breast, lung and colorectal cancer (15). Its mechanisms of action include the induction of apoptosis, necroptosis and immunogenic cell death, as well as the inhibition of angiogenesis and key signaling pathways, such as EGFR and PI3K/Akt (27,28). Shikonin also enhances the efficacy of conventional therapies by sensitizing cancer cells to chemotherapy and radiotherapy (28,29). However, its clinical application is limited by poor stability, low bioavailability and potential toxicity to normal cells (29). Acetylshikonin, a shikonin derivative, overcomes these limitations and demonstrates potential as a more effective candidate for cancer treatment. The acetylation of shikonin enhances its stability and bioavailability, facilitating more effective delivery and sustained action within the body (15). Acetylshikonin has been reported to trigger ROS-dependent apoptosis in hepatocellular carcinoma and to activate necroptosis via the RIPK1/RIPK3 signaling axis in lung cancer cells (16,30). However, most of these studies have predominantly focused on classical cell death pathways, and the role of acetylshikonin in ferroptosis has remained largely unexplored. The present findings provide novel evidence that acetylshikonin selectively induces ferroptosis in osteosarcoma cells by promoting lipid peroxidation, increasing intracellular Fe^{2+} levels and suppressing GPX4 expression. These results highlight a previously unrecognized mechanism for acetylshikonin, which could have important

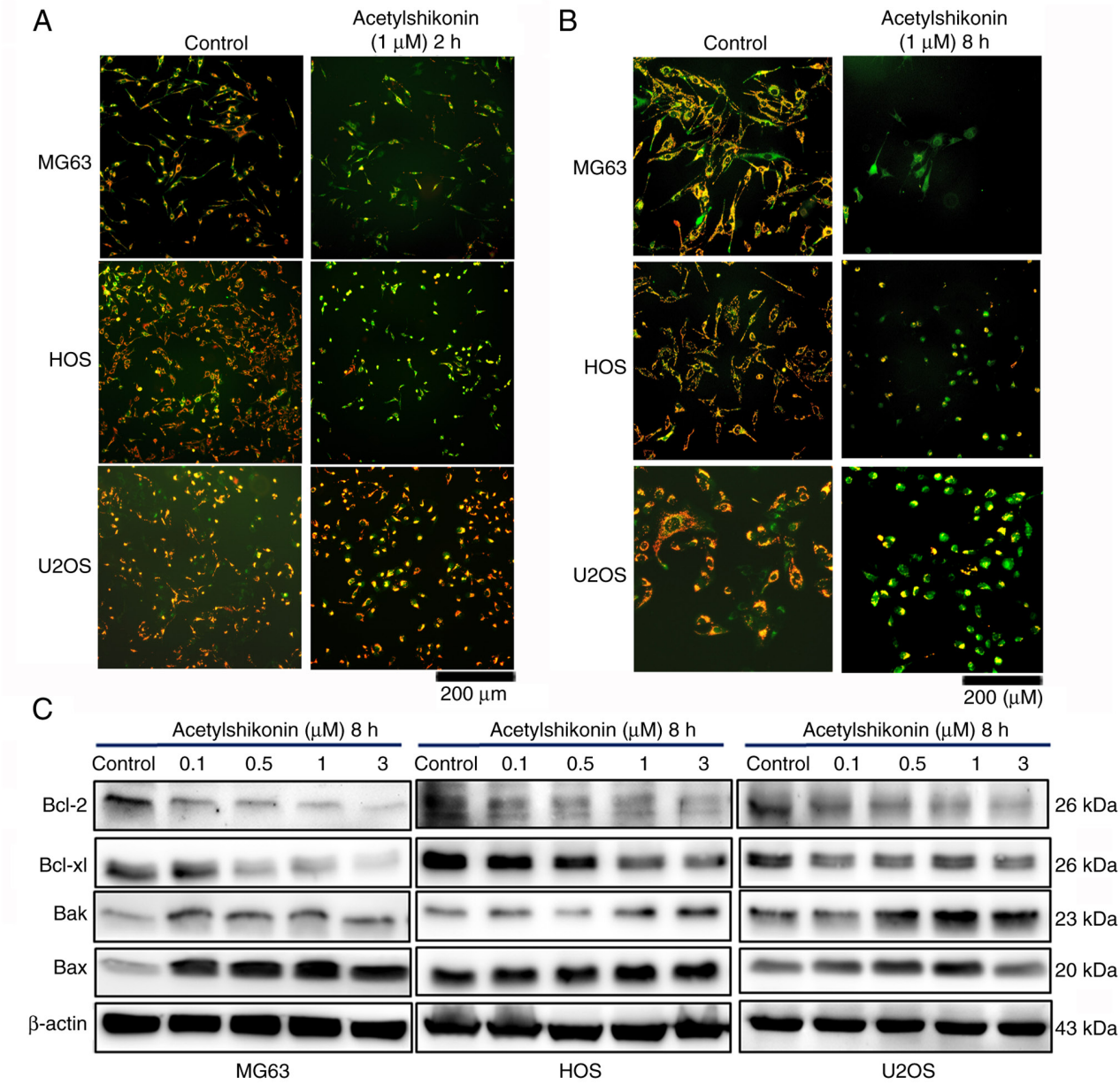

Figure 6. Acetylshikonin disrupts mitochondrial membrane potential. Cells were incubated with acetylshikonin (1 μM) for (A) 2 or (B) 8 h and subsequently stained with JC-1 (n=4). (C) Western blot analysis of Bcl-2, Bcl-xl, Bax and Bak protein expression in osteosarcoma cells following acetylshikonin treatment (0.1-3 μM) for 8 h (n=4). Untreated cells served as controls. Data are presented as the mean ± SD.

therapeutic implications in overcoming therapeutic resistance in osteosarcoma.

Although the present study primarily focused on the *in vitro* anticancer effects of acetylshikonin, several previous investigations have provided valuable insights into its pharmacokinetic characteristics. In radiolabeled mouse studies, [^{3}H]-acetylshikonin became detectable in plasma within 15 min of oral administration, with peak concentrations occurring at ~1 h. Notably, the compound showed widespread tissue distribution, particularly in the gastrointestinal tract and liver; however, it exhibited poor systemic absorption, with >80% of the administered dose recovered in feces within 48 h, suggesting limited bioavailability (31). Furthermore, acetylshikonin has demonstrated high plasma protein binding, and in mice, its parent form was reported to be undetectable in circulation, complicating direct pharmacokinetic analysis (30). In a non-human primate model, Sun *et al* (32) employed a derivatization-based liquid chromatography-electrospray ionization-tandem mass spectrometry assay, and revealed that oral administration of acetylshikonin resulted in a terminal half-life of 12.3±1.6 h and a mean residence time of 10.2±0.7 h, indicating prolonged systemic exposure. In terms of chemical stability, acetylshikonin has been reported to be relatively stable under acidic aqueous-organic conditions. For example, in pH 3.0 glycine buffer containing 50% ethanol, its half-life was measured as 67.0±9.6 h at 40˚C and 31.3±3.3 h at 70˚C (33). These findings suggest that while acetylshikonin demonstrates favorable chemical stability and residence time, its limited oral bioavailability remains a key limitation. Future *in vivo* studies should therefore focus on formulation strategies and structural modifications to enhance its absorption and therapeutic potential in osteosarcoma models.

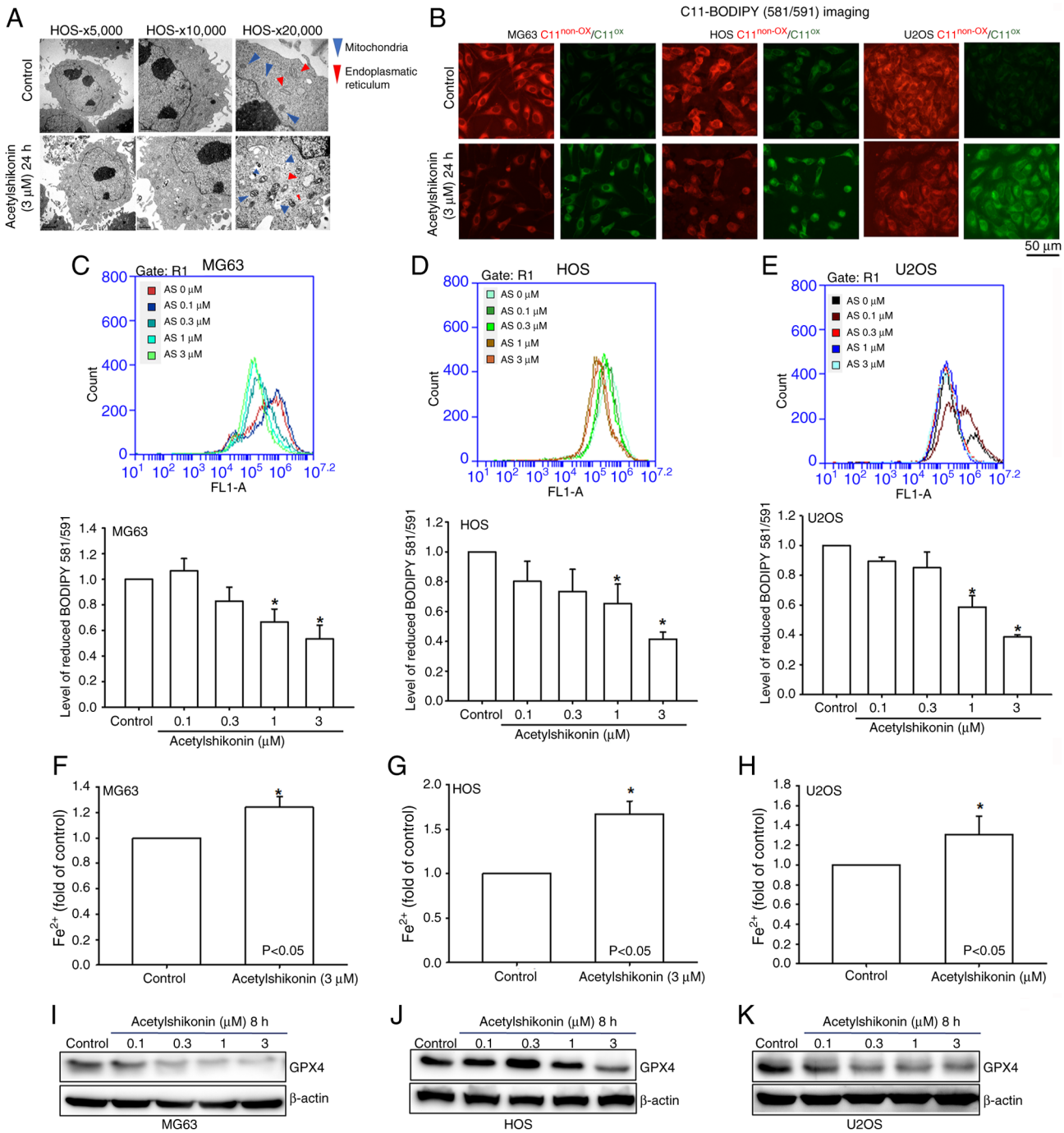

Figure 7. Acetylshikonin decreases mitochondrial volume and enhances lipid peroxidation in osteosarcoma cells. (A) Transmission electron microscopy images of HOS cells treated with acetylshikonin (3 μM) for 24 h, showing a reduction in mitochondrial volume (blue triangles). The red arrow indicates the endoplasmic reticulum. (B) Fluorescence microscopy analysis of lipid peroxidation in osteosarcoma cells treated with acetylshikonin (3 μM) and C11-BODIPY™ 581/591 (n=4). (C-E) Flow cytometric analyses showing lipid peroxidation in osteosarcoma cells incubated with acetylshikonin (0.1-3 μM) and C11-BODIPY (581/591) for 30 min (n=4). (F-H) Intracellular Fe^{2+} levels in osteosarcoma cells treated with acetylshikonin (3 μM) for 24 h were quantified using an Fe^{2+} detection reagent and microplate reader. (I-K) Western blot analysis of GPX4 protein expression in osteosarcoma cells treated with acetylshikonin (0.1-3 μM) for 8 h (n=4). Untreated cells served as controls. Data are presented as the mean ± SD. *P<0.05 vs. untreated control. GPX4, glutathione peroxidase 4; Fe^{2+}, ferrous ion.

The present study utilized U2OS, HOS and MG63 osteosarcoma cell lines, which represent diverse genetic profiles of osteosarcoma. In the HOS cell line, a TP53 mutation has been confirmed, classifying it as a p53-mutated cell line. Therefore, HOS represents a model of p53-mutated osteosarcoma with a functional RB pathway (34). The U2OS cell line is classified as p53 wild-type or expressing, maintaining functional p53 expression. It harbors a heterozygous BRCA2 mutation, with likely preservation of one intact allele, and shows reduced or absent RB1 protein expression, suggesting a defective RB pathway. Thus, U2OS exhibits partial BRCA2 deficiency combined with a compromised RB pathway (34,35). MG63 cells are characterized by a complete absence of TP53 (classified as p53-null), and markedly reduced or absent RB1 protein expression. This cell line demonstrates genomic instability, homologous recombination deficiency, loss of heterozygosity

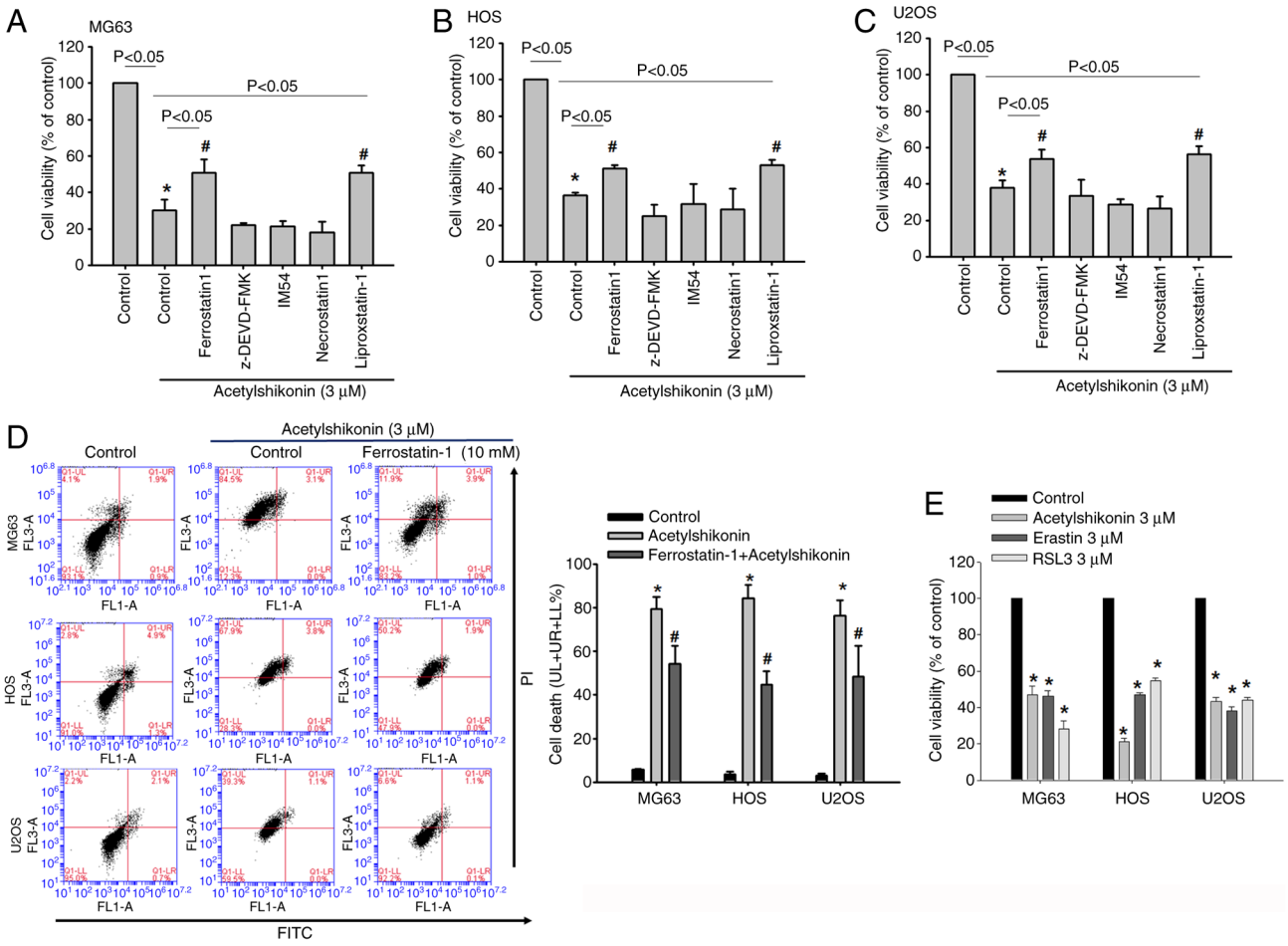

Figure 8. Acetylshikonin induces ferroptosis-mediated cell death. (A-C) CCK-8 assay results of osteosarcoma cells pretreated with ferrostatin-1 (10 μM), z-DEVD-FMK (10 μM), necrostatin-1 (10 μM), IM54 (10 μM) and liproxstain-1 (1 μM) for 1 h before exposure to acetylshikonin (3 μM) for 24 h (n=4). (D) Flow cytometric analysis of Annexin V/PI staining in osteosarcoma cells pretreated with ferrostatin-1 (10 μM) for 1 h followed by acetylshikonin (3 μM) for 24 h (n=4). (E) CCK-8 assay results of osteosarcoma cells treated with acetylshikonin (3 μM), erastin (3 μM) and RSL3 (3 μM) for 24 h (n=4). Untreated cells served as controls. Data are presented as the mean ± SD. *P<0.05 vs. untreated control; #P<0.05 vs. acetylshikonin-treated group. CCK-8, Cell Counting Kit-8.

and a 'BRCAness' phenotype, typical of BRCA1/2-mutant tumors, marked by disruptive alterations in DNA repair pathways (34,35). While these cell lines model varying degrees of tumor aggressiveness and genetic alterations, they may not fully capture the molecular diversity of clinical osteosarcoma subtypes, particularly those with metastatic or drug-resistant phenotypes. To address this limitation, future studies should include additional cell lines, such as SJSA-1 (TP53-mutated, highly invasive) and 143B (a metastatic HOS derivative with enhanced migratory capacity), to better evaluate the therapeutic potential of acetylshikonin across diverse osteosarcoma subtypes.

From a clinical perspective, the present findings suggest that acetylshikonin could serve as a promising complementary agent in osteosarcoma treatment. In traditional Chinese medicine, natural compounds are often used alone or in combination with Western therapies to enhance antitumor efficacy and reduce treatment-related toxicity. The integration of natural products into conventional treatment regimens is gaining increasing attention in oncology (36-38). Given the substantial side effects and the frequent emergence of drug resistance associated with current standard chemotherapies for osteosarcoma, including doxorubicin, cisplatin and high-dose methotrexate, the introduction of a ferroptosis-inducing agents such as acetylshikonin may provide synergistic benefits (39,40). Specifically, combining acetylshikonin with standard chemotherapeutic agents could enhance therapeutic effectiveness by simultaneously activating multiple, non-redundant cell death pathways. Moreover, the minimal toxicity of acetylshikonin toward normal osteoblasts, as observed in the present study, supports its feasibility as an adjunctive treatment strategy.

To provide a broader context, the present findings may be compared with those of previous studies on the anticancer effects of acetylshikonin. Prior studies have demonstrated that acetylshikonin induces apoptosis in hepatocellular carcinoma and triggers necroptosis through the RIPK1/RIPK3 pathway in lung cancer cells (15,30). However, its role in ferroptosis has remained largely uncharacterized. The current study is among the first to show that acetylshikonin may promote ferroptosis in osteosarcoma cells by enhancing lipid peroxidation, increasing intracellular Fe^{2+} concentrations and downregulating GPX4 expression, representing a novel mechanistic contribution to the understanding of this compound (10,11,41). To assess clinical feasibility, previous reports have highlighted the limitations

of high-dose MAP regimens (methotrexate, doxorubicin and cisplatin) in metastatic or recurrent osteosarcoma, and have identified iron metabolism as a targetable vulnerability associated with ROS production and tumor resistance (39,42,43). Furthermore, curcumin enhances methotrexate efficacy by suppressing the Hedgehog signaling pathway, thereby overcoming resistance and reducing proliferation (39). Based on these insights, acetylshikonin may represent a potential complementary agent to activate non-redundant cell death pathways, warranting future investigation into its synergistic potential with conventional chemotherapeutics.

In summary, the present study highlights acetylshikonin, a naphthoquinone derivative, as a promising therapeutic candidate for osteosarcoma. Acetylshikonin reduced osteosarcoma cell viability and selectively promoted ferroptosis by increasing ROS production, disrupting mitochondrial function, enhancing lipid peroxidation, downregulating GPX4 and elevating intracellular iron levels. These findings suggest that acetylshikonin may help overcome therapeutic resistance and improve outcomes in osteosarcoma. Future studies should evaluate its efficacy *in vivo*, explore its potential in combination with standard chemotherapy agents, and assess its pharmacokinetic and safety profiles to facilitate clinical translation.

Acknowledgements

Not applicable.

Funding

This work was supported by a grant from the National Science and Technology Council of Taiwan (NSTC113-2628-B-038-008-MY3).

Availability of data and materials

The data generated in the present study may be requested from the corresponding author.

Authors' contributions

JYC was responsible for data collection, conceptualization, methodology development, investigation and preparation of the original draft. GSW contributed to conceptualization, project administration, investigation and software analysis. TMC performed formal analysis, contributed to methodology and project administration, and conducted software analysis. JFL conceptualized the study, developed the methodology, performed investigation, collected data, acquired funding, and critically reviewed and edited the manuscript. TMC and JFL confirm the authenticity of all the raw data. All authors read and approved the final manuscript.

Ethics approval and consent to participate

Not applicable.

Patient consent for publication

Not applicable.

Competing interests

The authors declare that they have no competing interests.

References

1. Ottaviani G and Jaffe N: The epidemiology of osteosarcoma. Cancer Treat Res 152: 3-13, 2009.
2. Meltzer PS and Helman LJ: New Horizons in the treatment of osteosarcoma. N Engl J Med 385: 2066-2076, 2021.
3. Belayneh R, Fourman MS, Bhogal S and Weiss KR: Update on osteosarcoma. Curr Oncol Rep 23: 71, 2021.
4. Lilienthal I and Herold N: Targeting molecular mechanisms underlying treatment efficacy and resistance in osteosarcoma: A review of current and future strategies. Int J Mol Sci 21: 6885, 2020.
5. Haider T, Pandey V, Banjare N, Gupta PN and Soni V: Drug resistance in cancer: Mechanisms and tackling strategies. Pharmacol Rep 72: 1125-1151, 2020.
6. Mohammad RM, Muqbil I, Lowe L, Yedjou C, Hsu HY, Lin LT, Siegelin MD, Fimognari C, Kumar NB, Dou QP, *et al*: Broad targeting of resistance to apoptosis in cancer. Semin Cancer Biol 35 (Suppl 1): S78-S103, 2015.
7. Wang J, Li M, Guo P and He D: Correction: Survival benefits and challenges of adjuvant chemotherapy for high-grade osteosarcoma: A population-based study. J Orthop Surg Res 18: 834, 2023.
8. Hiraga H and Ozaki T: Adjuvant and neoadjuvant chemotherapy for osteosarcoma: JCOG bone and soft tissue tumor study group. Jpn J Clin Oncol 51: 1493-1497, 2021.
9. Zhang C, Liu X, Jin S, Chen Y and Guo R: Ferroptosis in cancer therapy: A novel approach to reversing drug resistance. Mol Cancer 21: 47, 2022.
10. Zhou N and Bao J: FerrDb: A manually curated resource for regulators and markers of ferroptosis and ferroptosis-disease associations. Database (Oxford) 2020: baaa021, 2020.
11. Zhou Q, Meng Y, Li D, Yao L, Le J, Liu Y, Sun Y, Zeng F, Chen X and Deng G: Ferroptosis in cancer: From molecular mechanisms to therapeutic strategies. Signal Transduct Target Ther 9: 55, 2024.
12. Nie Q, Hu Y, Yu X, Li X and Fang X: Induction and application of ferroptosis in cancer therapy. Cancer Cell Int 22: 12, 2022.
13. Wu Y, Yu C, Luo M, Cen C, Qiu J, Zhang S and Hu K: Ferroptosis in cancer treatment: Another way to rome. Front Oncol 10: 571127, 2020.
14. Hayashi M: Pharmacological studies of Shikon and Tooki. (2) Pharmacological effects of the pigment components, Shikonin and acetylshikonin. Nihon Yakurigaku Zasshi 73: 193-203, 1977 (In Japanese).
15. Wang Q, Wang J, Wang J, Ju X and Zhang H: Molecular mechanism of shikonin inhibiting tumor growth and potential application in cancer treatment. Toxicol Res (Camb) 10: 1077-1084, 2021.
16. Hu S, Li Y, Zhou J, Xu K, Pang Y, Weiskirchen R, Ocker M and Ouyang F: Identification of acetylshikonin as a novel tubulin polymerization inhibitor with antitumor activity in human hepatocellular carcinoma cells. J Gastrointest Oncol 14: 2574-2586, 2023.
17. Cha HS, Lee HK, Park SH and Nam MJ: Acetylshikonin induces apoptosis of human osteosarcoma U2OS cells by triggering ROS-dependent multiple signal pathways. Toxicol In Vitro 86: 105521, 2023.
18. Majtnerova P and Rousar T: An overview of apoptosis assays detecting DNA fragmentation. Mol Biol Rep 45: 1469-1478, 2018.
19. Loo DT: TUNEL assay. An overview of techniques. Methods Mol Biol 203: 21-30, 2002.
20. Wang B, Wang Y, Zhang J, Hu C, Jiang J, Li Y and Peng Z: ROS-induced lipid peroxidation modulates cell death outcome: Mechanisms behind apoptosis, autophagy, and ferroptosis. Arch Toxicol 97: 1439-1451, 2023.
21. Rizwan H, Pal S, Sabnam S and Pal A: High glucose augments ROS generation regulates mitochondrial dysfunction and apoptosis via stress signalling cascades in keratinocytes. Life Sci 241: 117148, 2020.
22. Battaglia AM, Chirillo R, Aversa I, Sacco A, Costanzo F and Biamonte F: Ferroptosis and cancer: Mitochondria meet the 'Iron Maiden' cell death. Cells 9: 1505, 2020.
23. Fu B, Lou Y, Wu P, Lu X and Xu C: Emerging role of necroptosis, pyroptosis, and ferroptosis in breast cancer: New dawn for overcoming therapy resistance. Neoplasia 55: 101017, 2024.

24. Sajeev A, Sailo B, Unnikrishnan J, Talukdar A, Alqahtani MS, Abbas M, Alqahtani A, Sethi G and Kunnumakkara AB: Unlocking the potential of Berberine: Advancing cancer therapy through chemosensitization and combination treatments. Cancer Lett 597: 217019, 2024.
25. Chen X, Comish PB, Tang D and Kang R: Characteristics and biomarkers of ferroptosis. Front Cell Dev Biol 9: 637162, 2021.
26. Chen F, Kang R, Tang D and Liu J: Ferroptosis: Principles and significance in health and disease. J Hematol Oncol 17: 41, 2024.
27. Yadav S, Sharma A, Nayik GA, Cooper R, Bhardwaj G, Sohal HS, Mutreja V, Kaur R, Areche FO, AlOudat M, *et al*: Review of shikonin and derivatives: Isolation, chemistry, biosynthesis, pharmacology and toxicology. Front Pharmacol 13: 905755, 2022.
28. Iranzadeh S, Dalil D, Kohansal S and Isakhani M: Shikonin in breast cancer treatment: A comprehensive review of molecular pathways and innovative strategies. J Pharm Pharmacol 76: 967-982, 2024.
29. Qi K, Li J, Hu Y, Qiao Y and Mu Y: Research progress in mechanism of anticancer action of shikonin targeting reactive oxygen species. Front Pharmacol 15: 1416781, 2024.
30. Lin SS, Chang TM, Wei AI, Lee CW, Lin ZC, Chiang YC, Chi MC and Liu JF: Acetylshikonin induces necroptosis via the RIPK1/RIPK3-dependent pathway in lung cancer. Aging (Albany NY) 15: 14900-14914, 2023.
31. Zhang Z, Bai J, Zeng Y, Cai M, Yao Y, Wu H, You L, Dong X and Ni J: Pharmacology, toxicity and pharmacokinetics of acetylshikonin: A review. Pharm Biol 58: 950-958, 2020.
32. Sun DX, Tian HF, Meng ZY, Du A, Yuan D, Gu RL, Wu ZN and Dou GF: Quantitative determination of acetylshikonin in macaque monkey blood by LC-ESI-MS/MS after precolumn derivatization with 2-mercaptoethanol and its application in pharmacokinetic study. Acta Pharmacol Sin 29: 1499-1506, 2008.
33. Cho MH, Paik YS and Hahn TR: Physical stability of shikonin derivatives from the roots of Lithospermum erythrorhizon cultivated in Korea. J Agric Food Chem 47: 4117-4120, 1999.
34. Zhang Q, Hao S, Wei G, Liu X and Miao Y: The p53-mediated cell cycle regulation is a potential mechanism for emodin-suppressing osteosarcoma cells. Heliyon 10: e26850, 2024.
35. Engert F, Kovac M, Baumhoer D, Nathrath M and Fulda S: Osteosarcoma cells with genetic signatures of BRCAness are susceptible to the PARP inhibitor talazoparib alone or in combination with chemotherapeutics. Oncotarget 8: 48794-48806, 2017.
36. Wei J, Liu Z, He J, Liu Q, Lu Y, He S, Yuan B, Zhang J and Ding Y: Traditional Chinese medicine reverses cancer multidrug resistance and its mechanism. Clin Transl Oncol 24: 471-482, 2022.
37. Miao K, Liu W, Xu J, Qian Z and Zhang Q: Harnessing the power of traditional Chinese medicine monomers and compound prescriptions to boost cancer immunotherapy. Front Immunol 14: 1277243, 2023.
38. Yuan J, Liu Y, Zhang T, Zheng C, Ding X, Zhu C, Shi J and Jing Y: Traditional Chinese medicine for breast cancer treatment: A bibliometric and visualization analysis. Pharm Biol 62: 499-512, 2024.
39. Argenziano M, Tortora C, Pota E, Di Paola A, Di Martino M, Di Leva C, Di Pinto D and Rossi F: Osteosarcoma in children: Not only chemotherapy. Pharmaceuticals (Basel) 14: 923, 2021.
40. Giliberti G, Marrapodi MM, Di Feo G, Pota E, Di Martino M, Di Pinto D, Rossi F and Di Paola A: Curcumin and methotrexate: A promising combination for osteosarcoma treatment via hedgehog pathway inhibition. Int J Mol Sci 25: 11300, 2024.
41. Hsu PC, Tsai CC, Lin YH and Kuo CY: Therapeutic targeting of apoptosis, autophagic cell death, necroptosis, pyroptosis, and ferroptosis pathways in oral squamous cell carcinoma: Molecular mechanisms and potential strategies. Biomedicines 13: 1745, 2025.
42. Ma X, Zhao J and Feng H: Targeting iron metabolism in osteosarcoma. Discov Oncol 14: 31, 2023.
43. Zhao J, Zhao Y, Ma X, Zhang B and Feng H: Targeting ferroptosis in osteosarcoma. J Bone Oncol 30: 100380, 2021.